

Phase Diagrams of Water and Sodium Dodecyl Sulfate Combined with Four Commercial Nonionic Surfactants

S.E. Friberg* and M. Chiu

Center for Advanced Materials Processing and Department of Chemistry, Clarkson University, Potsdam, New York 13699-5814

Phase diagrams in which water was combined with sodium dodecyl sulfate, plus one of four nonionic surfactants, as well as an aliphatic oil, were determined by visual observation and low-angle X-ray diffractometry. The results agreed with earlier investigations on specially synthesized polyethyleneglycol alkyl ether surfactants, except that the extended water-in-oil microemulsion areas were not found with the commercial surfactants.

KEY WORDS: Detergents, liquid crystals, micelles, microemulsions, phase equilibria.

Mixtures of anionic and nonionic surfactants are frequently formulated for commercial applications, and their properties in aqueous systems have been investigated extensively (1-7). These studies are important to better understand solubilization in aqueous systems, as well as stability of traditional two-phase emulsions and foams.

However, mixed surfactant systems have revealed some unexpected phenomena in the stabilization of microemulsions (8). They prompted an investigation of all the phase regions in systems comprised of an ionic surfactant, nonionic surfactants of the polyethyleneglycol alkyl ether type and water (9). The results showed that the behavior of the nonionic surfactant depended on the length of its polar chain. With a low number of oxyethylene groups (9), the nonionic surfactant acted as a powerful cosurfactant and stabilized the lamellar liquid crystal in the system. Nonionic surfactants with long polar chains showed a phase behavior indistinguishable from that of the ionic surfactant. Such surfactant combinations have recently been shown to have a pronounced effect on adsorption behavior as revealed by Sjöblom and co-workers (10,11) and Saeten *et al.* (12).

The results were valid for specially synthesized compounds in which all the molecules had the same number of oxyethylene groups. The investigation on microemulsions indicated that the purity in terms of the polar chain-length has a decisive influence on properties and, thus, an investigation was initiated to evaluate similar systems with commercial nonionic surfactant combinations.

In the present article we present results obtained with sodium dodecyl sulfate and commercial surfactants with different polar chainlengths.

EXPERIMENTAL PROCEDURES

Materials. Sodium dodecyl sulfate (SDS) (BDH Chemical Ltd., Poole, England; specially pure) was recrystallized twice from absolute ethanol. Surfactants triethyleneglycoldodecylether (TGDE) and pentaethyleneglycoldodecylether (PGDE, II) (55-100%) were commercial products from Shell Chemical Co. (Houston, TX). The solvents were removed from the surfactants prior to use, and triethyleneglycolnonylphenoether (TEGNPE) and penta-

ethyleneglycolnonylphenoether (PGDEI), from GAF Chemical Co. (Newark, NJ) were used without change. Isopar M (98% paraffins including naphthenes) was from Chevron Environmental Health Center (Newark, NJ). Water was twice distilled.

Determination of phase diagrams. The isotropic solution regions were determined by adding one component to a mixture of the other compounds while noting transparency for the isotropic solutions. The compositions were thermostatted at 25°C for three days to ensure no significant changes of solubility.

The lamellar, normal hexagonal, inverse hexagonal and isotropic (or cubic) liquid crystal regions were identified by visual observation between polarized films and between crossed polarizers in a microscope. Their extensions were confirmed by small-angle X-ray diffraction observing breaks in the interlayer spacing curves *vs.* solvent content.

RESULTS

SDS/water + (TGDE) and + (TEGNPE). The phase diagrams of water and sodium dodecyl sulfate (SDS) combined with TGDE and with TEGNPE are given in Figures 1 and 2. Two isotropic liquid phases, L_1 and L_2 , were found for both surfactants. L_1 , emanating from the water corner, is an aqueous micellar solution solubilizing the nonionic surfactant. The nonionic surfactant solution dissolved water to 19% TGDE, but the ionic surfactant dissolved water only to an insignificant level. SDS was not significantly soluble in TGDE, but addition of water to a water/ionic surfactant molar ratio of 8 increased the SDS solubility in TGDE to 20% by weight. No increase in water solubility in TGDE was found when SDS was added to it. On the contrary, the water solubility was reduced to 9% for the maximum SDS content (Fig. 1). On the other hand, the water solubility in TEGNPE was strongly increased from 0 to 22.5% by weight with addition of SDS.

At surfactant concentrations in excess of those in the aqueous micellar solution L_1 , a liquid crystalline phase, E, was found with a structure of hexagonally arranged cylinders. Increased fraction of the nonionic surfactant gave a lamellar liquid crystalline region, D, located between 18 and 50% by weight for water content, and a range of ionic surfactant/nonionic surfactant fraction of 25-70% for TGDE. TEGNPE displayed the lamellar liquid crystal at lower nonionic surfactant/SDS ratios and, in addition, gave an inverse hexagonal phase, F, with a minimum water/surfactant molecular ratio of 4.

The two-phase area at low SDS content was narrow, reaching 1.0% SDS at high nonionic surfactant content, and 5% SDS at high water content for TGDE. The ensuing three-phase area was connected to the maximum water content composition of the crystalline phase. The TEGNPE system required higher SDS content for the three-phase region and, in addition, another three-phase region was found involving the L_2 liquid phase plus the two liquid crystals.

*To whom correspondence should be addressed.

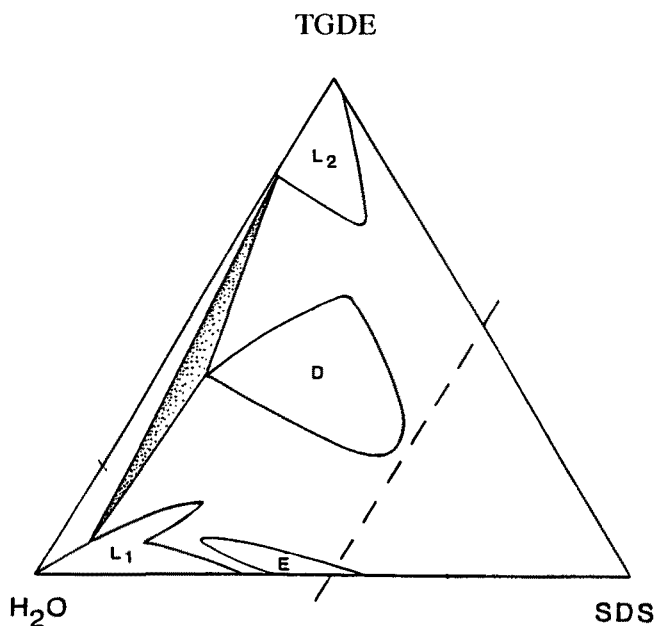


FIG. 1. Partial phase diagram for the system of water (H_2O), SDS + triethyleneglycoldodecylether (TGDE). L_1 , aqueous micellar solution; L_2 , nonionic surfactant solution; E, normal hexagonal liquid crystal; and D, lamellar liquid crystal.

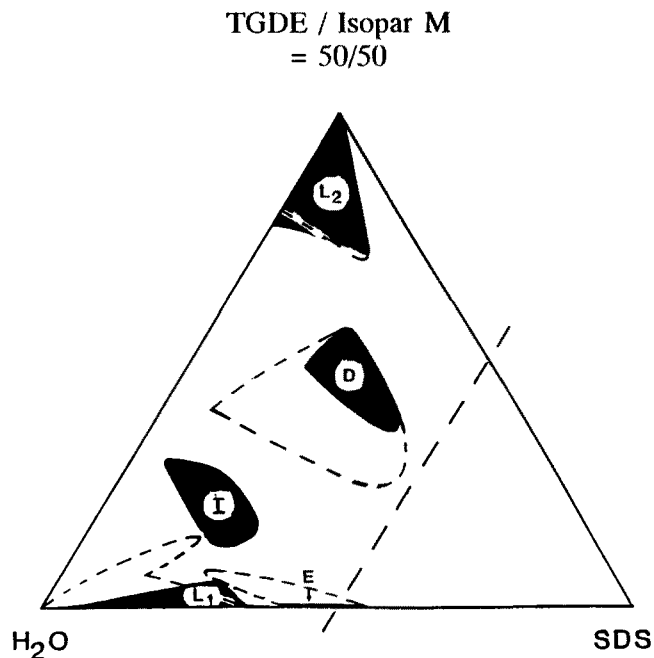


FIG. 3. System of Figure 1 (dashed lines), but with the nonionic surfactant replaced by a 1:1 weight ratio of the nonionic surfactant and the oil, Isopar M (filled areas).

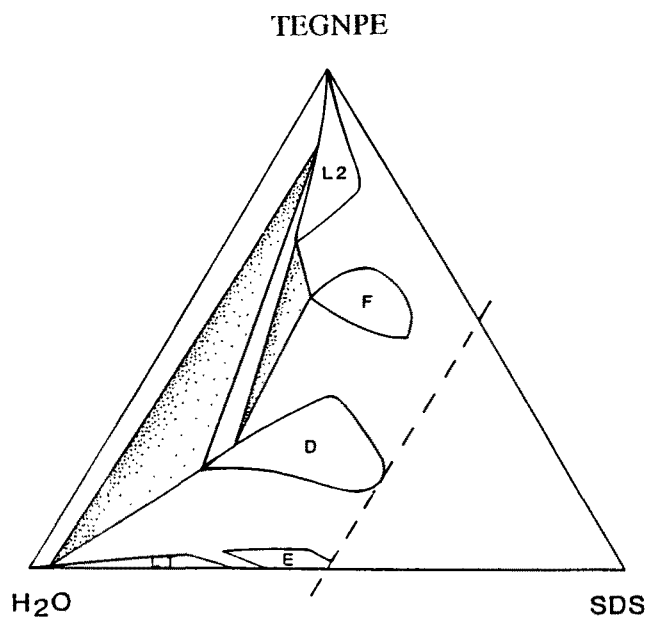


FIG. 2. Partial phase diagram for the system of water, SDS and triethyleneglycolnonylphenoether (TEGNPE). Abbreviations as in Figure 1. F = inverse hexagonal liquid crystal.

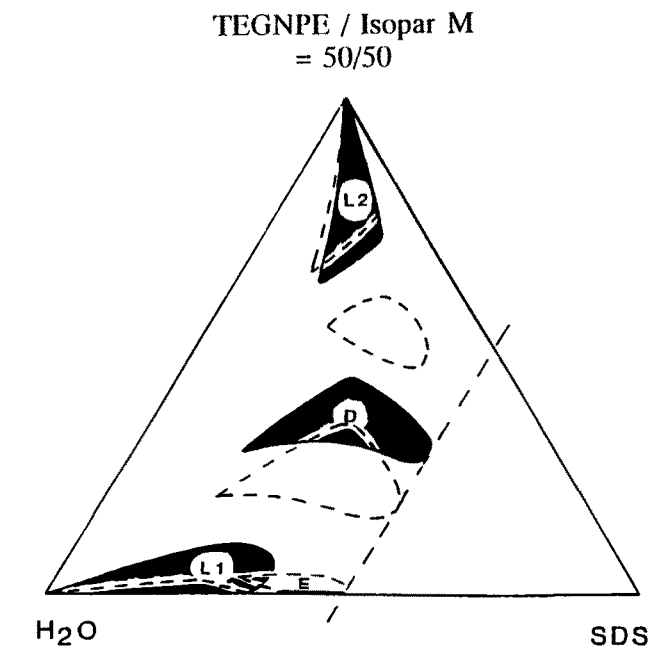


FIG. 4. System of Figure 2 (dashed lines), but with the nonionic surfactant replaced by a 1:1 weight ratio of the nonionic surfactant and the oil, Isopar M (filled areas).

Isopar M/SDS/water + TGDE and + TEGNPE. Fifty percent substitution of nonionic surfactant by the hydrocarbon, Isopar M, led to phase diagrams shown in Figures 3 and 4 (black areas). In the micellar solution region, the maximum solubilization of TGDE and hydrocarbon was reduced to 5% by weight, and an isotropic liquid

crystal was formed. The TEGNPE combination instead gave enhanced solubilization.

The nonionic surfactant/Isopar M solution areas (L_2) of Figures 3 and 4 were approximately identical to those without hydrocarbon (Figs. 1 and 2). The areas for the lamellar and normal hexagonal liquid crystals were also

PHASE DIAGRAMS OF WATER AND SDS

similar. In both cases, the lamellar liquid crystalline region was moved toward a higher nonionic surfactant/SDS ratio, and the solubilization into the normal hexagonal liquid crystal was strongly reduced.

SDS/water + PGDE, I and + PGDE, II. The phase regions in the three-component system SDS-water-PGDE, I and SDS-water-PGDE, II are shown in Figures 5 and 6.

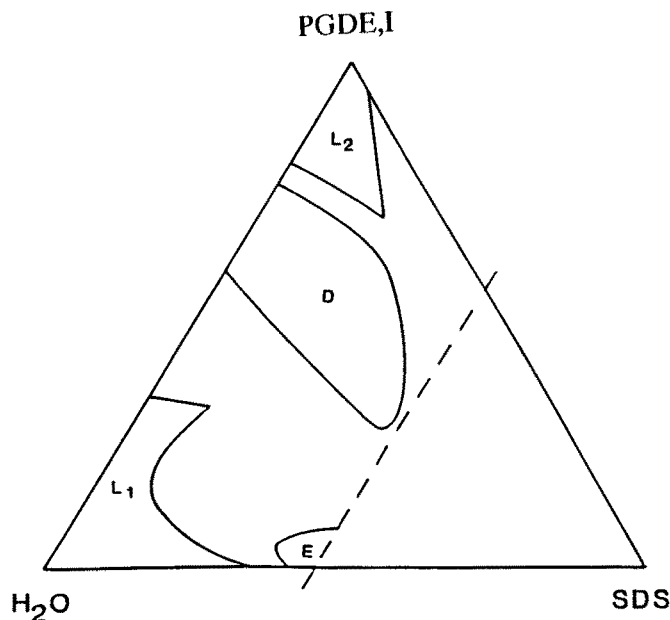


FIG. 5. Partial phase maps of the system water (H_2O), SDS + pentaethyleneglycoldodecylether (PGDE, I). L_1 = aqueous micellar solution, L_2 = nonionic surfactant solution, E = normal hexagonal liquid crystal, D = lamellar liquid crystal.

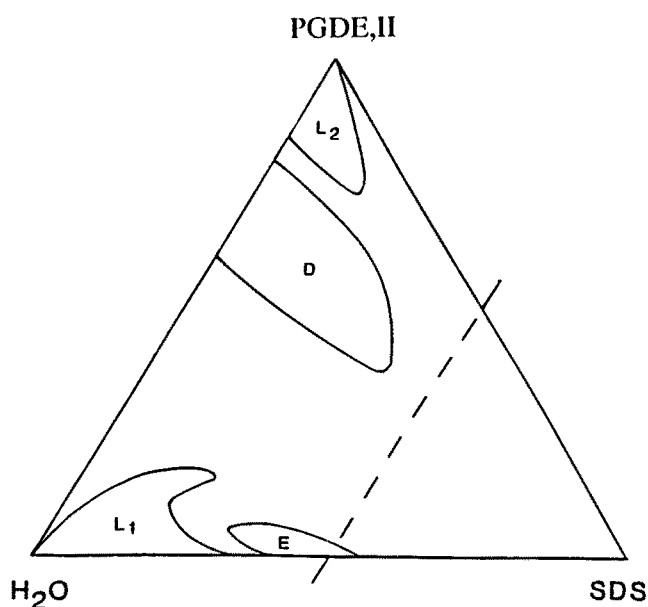


FIG. 6. Partial phase maps of the system water, SDS and PGDE, II. Abbreviations as in Figure 1.

The two phase diagrams are almost identical, with the lamellar liquid crystal occupying a large area limited by constant minimum and maximum water percentages and a minimum water/ionic surfactant ratio. The normal hexagonal liquid crystal, E, occupied a small area. The solubility into the water was extensive for PGDE, I (34% by weight), while PGDE, II was not soluble. Solubilization of the nonionic surfactant into the aqueous micellar solution of SDS was extensive.

PGDE, I/Isopar M/SDS/water. When the nonionic surfactant, PGDE, I, was substituted by equal amounts of hydrocarbon, Isopar M, the phase regions were changed drastically (Fig. 7). The aqueous micellar solution area L_1 and normal hexagonal liquid crystalline area E solubilized extremely small amounts of the hydrocarbon/PGDE, I solution. The size of the lamellar liquid crystalline region was strongly reduced and covered a water concentration range from 20–23% by weight. The PGDE, I/Isopar M solution region L_2 also was lessened. The PGDE, II surfactant was not soluble in the hydrocarbon, Isopar M, at the 1:1 ratio.

Small-angle X-ray measurements. Figures 8–11 show interlayer spacings of the lamellar liquid crystalline phases of the different systems at varied ionic surfactant/nonionic surfactant weight ratios. The TGDE and TEGNPE systems gave interlayer spacings, d_0 (d extrapolated to zero water content), which were independent of the ionic/nonionic surfactant ratios. The increase of interlayer spacing with water content was reduced significantly with enhanced SDS/nonionic surfactant ratio for the TGDE system (Fig. 8), but remained constant for the TEGNPE system (Fig. 9). Replacing one-half of the nonionic surfactant by the oil gave the expected changes in d_0 , but little modification of the slopes (Figs. 10 and 11). Surfactants with longer polar chains gave similar interlayer

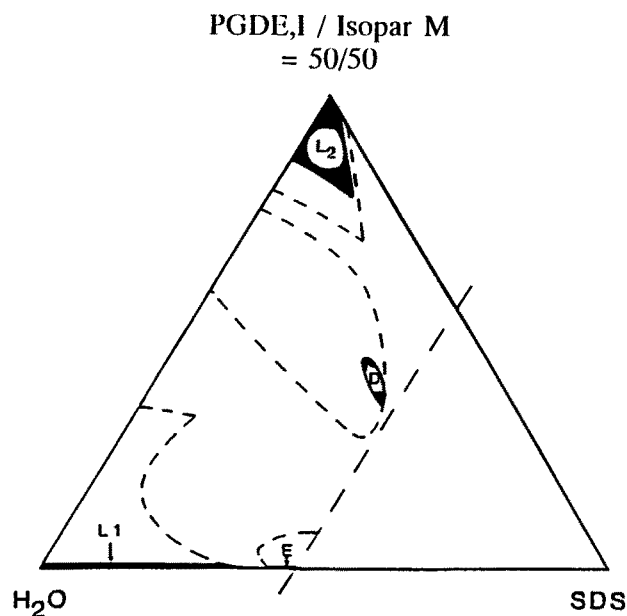


FIG. 7. Phase map of the system water (H_2O), SDS and pentaethyleneglycoldodecylether (PGDE, I)/Isopar M (1:1 weight ratio), filled parts. For comparison, the phases without hydrocarbon have been added (dashed lines).

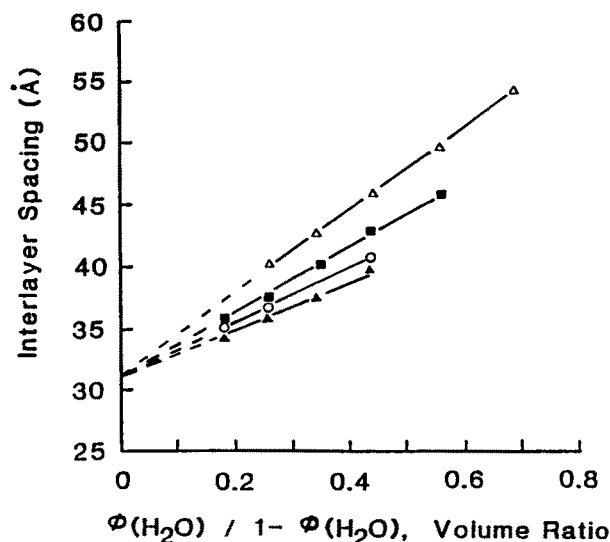


FIG. 8. Interlayer spacings for the lamellar phase (D) in Figure 1. SDS/TGDE, (Δ), 30:70; (\blacksquare), 40:60; (\circ), 50:50; and (\blacktriangle), 60:40.

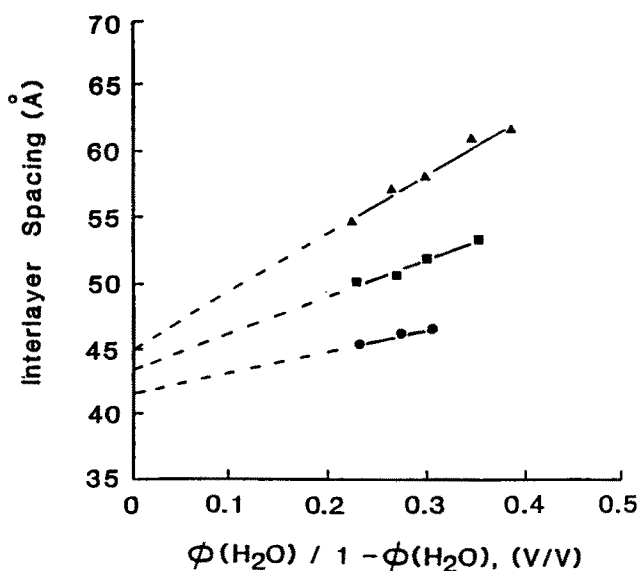


FIG. 10. Interlayer spacings for the lamellar phase (D) in Figure 3. SDS/TGDE-Isopar M, (Δ), 30:70; (\blacksquare), 40:60; and (\bullet), 50:50.

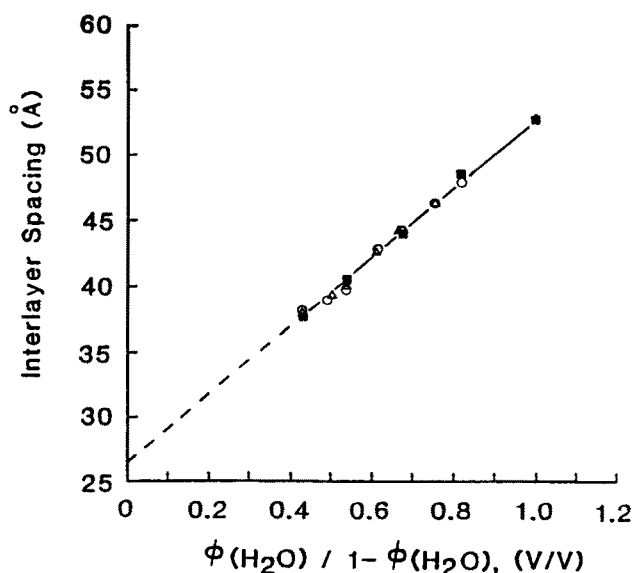


FIG. 9. Interlayer spacings for the lamellar phase (D) in Figure 2. SDS/TEGPE, (Δ), 50:50; (\blacksquare), 60:40; and (\circ), 70:30.

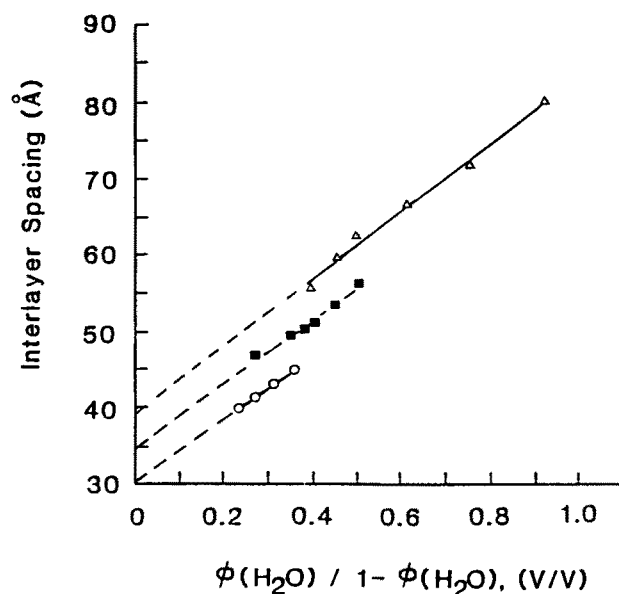


FIG. 11. Interlayer spacings for the lamellar phase (D) in Figure 4. SDS/TEGNPE-Isopar M, (Δ), 40:60; (\blacksquare), 50:50; and (\circ), 60:40.

spacing results (Figs. 12 and 13). The only difference is the slightly lower value for PGDEI.

DISCUSSION

The results are of interest both by themselves and in comparison with earlier results on well-defined nonionic surfactants (8,9). The series with TGDE corresponds to the system with $C_{12}EO_4$, except that the lamellar liquid crystal region is smaller for the TGDE. We assume this to be due to the variation in polar chainlength. Even a lamellar liquid crystal of a well-defined nonionic surfactant shows significant staggering along the molecular direction (13), resulting in order parameters close to the

lower limit for stability. With this result in mind, it appears reasonable that a commercial, nonionic surfactant with a significant polydispersity of the polar chainlength should show less stability against increased water content.

Addition of hydrocarbon did not lead to an increase of L_2 to form a water-in-oil (w/o) microemulsion region, as was the case for $C_{12}EO_4$ (8). It seems that the requirement for exact polar chainlength is extremely rigorous for a long-chain compound to serve as a cosurfactant for a w/o microemulsion, in accordance with earlier results (8).

The formation of a cubic liquid crystalline phase is in accordance with the results by Ekwall (14), who found such a phase when adding hydrocarbon to a water/sodium

PHASE DIAGRAMS OF WATER AND SDS

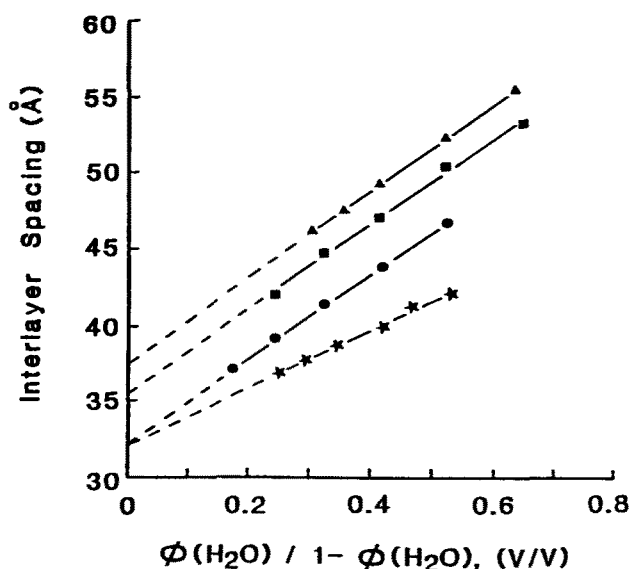


FIG. 12. Interlayer spacings in the lamellar (D) phase in Figure 5. SDS/PGDE, I, (▲), 0:100; (■), 10:90; (●), 30:70; and (★), 50:50.

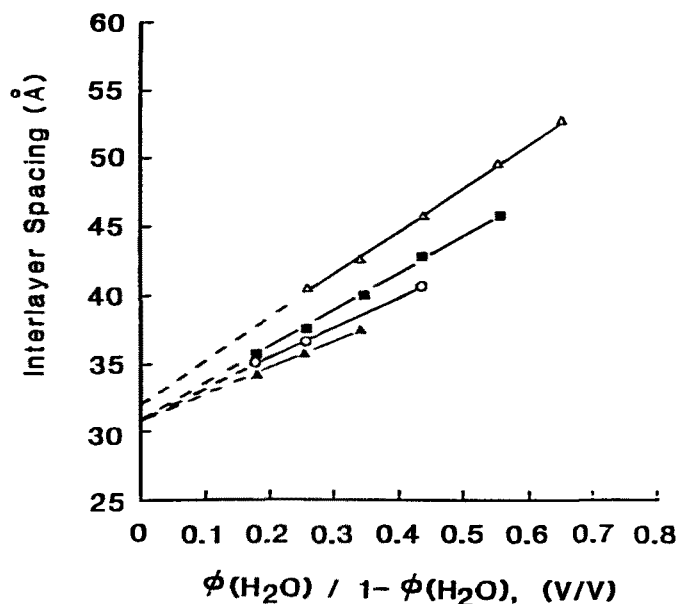


FIG. 13. Interlayer spacings in the lamellar (D) phase in Figure 6. SDS/PGDE, II, (Δ), 0:100; (■), 20:80; (○), 30:70; and (▲), 50:50.

octanoate system. The interlayer spacings from low-angle X-ray diffractograms leave information about the water penetration into the space between the surfactant hydrocarbon chains. The geometry of the liquid crystalline phase (Fig. 14) gives a relation between added water and interlayer spacing, provided no penetration takes place from zone A (Fig. 14) to zone B.

With this assumption, the contributions to interlayer spacings, d_w , are proportional to volume fractions ϕ_w . Hence:

$$d_s = k\phi_s \quad [1]$$

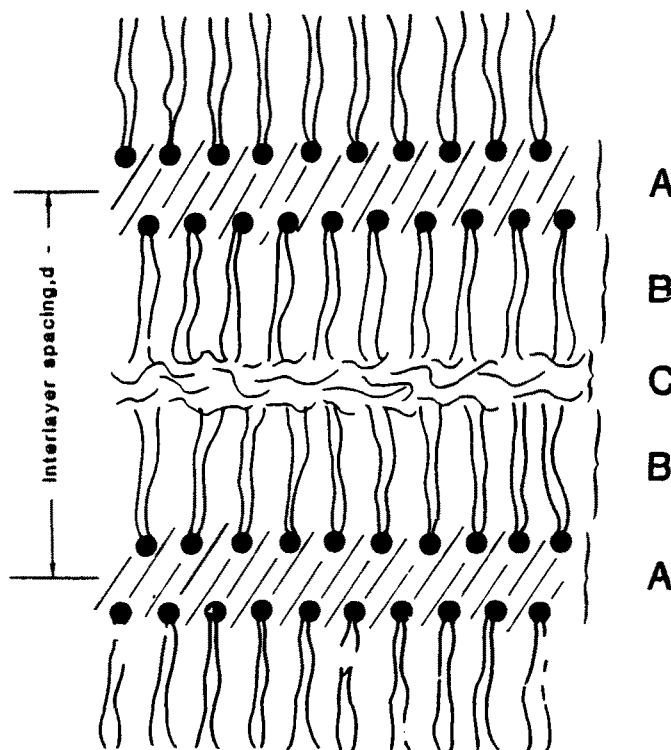


FIG. 14. In a lamellar crystal the water zone, A, is located between the polar groups. The amphiphiles form zone B, and C is located between the methyl groups of the latter.

$$d_w = k\phi_w \quad [2]$$

in which s denotes surfactant and w , water. Hence:

$$d_s/\phi_s = d_w/\phi_w \quad [3]$$

Furthermore,

$$d_s = d_0 \quad [4]$$

and the total interlayer spacing, d , is given by:

$$d = d_0 + d_w \quad [5]$$

$$d = d_0(1 + R) \quad [6]$$

in which $R = \phi_w/\phi_s$. The penetration fraction is defined by:

$$d = d_0[1 + (1-\alpha)R] \quad [7]$$

When $\alpha = 0$, there is no penetration and the water is localized to space A (Fig. 14). $\alpha = 1$ Means complete penetration; the water is evenly distributed along zone B (Fig. 14). When $\alpha = 0$, equation [7] changes to equation [6], while $\alpha = 1$ results in:

$$d = d_0 \quad [8]$$

The results in Tables 1-4 show several features that illuminate the differences between a hydrophobic surfactant, a headgroup with an aromatic ring (TEGNPE), and

TABLE 1

Interlayer Spacings Extrapolated to Zero Water Content, d_0 , and Water Penetration Fraction for the Lamellar Liquid Crystalline Phase in Water/SDS/TGDE and Water/SDS/TGDE-Isopar M Systems

	SDS/TGDE				SDS/TGDE-Isopar		
	30:70	40:60	50:50	60:40	30:70	40:60	50:50
d_0	30.0	30.0	30.0	30.0	45.0	43.7	41.5
Penetration %	13.4	22.6	26.2	41.1	3.0	38.5	59.8

TABLE 2

Interlayer Spacings Extrapolated to Zero Water Content, d_0 , and Water Penetration Fraction for the LC Phase in Water/SDS/TEGNPE and Water/SDS/TEGNPE-Isopar M Systems

	SDS/TEGNPE			SDS/TEGNPE-Isopar M		
	50:50	60:40	70:30	40:60	50:50	60:40
d_0	26.3	26.3	26.3	39.5	35.0	30.6
Penetration %	0.0	0.0	0.0	-10.5	-17.7	-30.1

TABLE 3

Interlayer Spacings Extrapolated to Zero Water Content, d_0 , and Water Penetration Fraction for the LC Phase in Water, PGDE, I Combined with SDS Systems

	SDS/PGDE, I			
	0:100	10:90	30:70	50:50
d_0	37.5	35.4	32.1	32.1
Penetration %	25.0	20.8	13.4	41.3

TABLE 4

Interlayer Spacings Extrapolated to Zero Water Content, d_0 , and Penetration Percent for LC Region in Water, SDS Combined with PGDE, II Systems

	SDS/PGDE, II			
	0:100	20:80	30:70	40:60
d_0	32.0	31.0	31.0	31.0
Penetration %	2.3	11.8	23.1	34.9

the corresponding headgroup without an aromatic ring (TGDE). The aromatic TEGNPE surfactant permitted no water penetration into the structure (Table 2), while TGDE showed high penetration, 41.1%, at an SDS weight ratio of 60:40 (Table 1). In addition, increasing the TGDE content gave a reduction in penetration.

We have no explanation for this difference, but would like to point out that the aromatic group of TEGNPE has a stronger interaction with a polar group than the purely aliphatic chain of TGDE. Hence, one should expect a

larger lateral force between SDS and the aromatic non-ionic surfactant than between SDS and the amphiphilic one. A stronger lateral force between the amphiphiles reduces water penetration, an experimental fact proven for the nonionic surfactants alone (11).

Addition of hydrocarbon resulted in a similar increase in extrapolated interlayer spacing (d_0) for low SDS/non-ionic surfactant ratios (Tables 1-4). On the other hand, high ratios gave only a small increase for the TGDE surfactant (Table 2). The ratio between the increase of interlayer spacing after addition of hydrocarbon and the hydrocarbon/nonhydrocarbon component volume ratio in the three columns to the right in Table 2 is of interest. The volume ratios were calculated by assuming a density of SDS equal to 1.0, of the nonionic surfactant equal to 0.9 and of Isopar M equal to 0.8. The ratios are 0.94, 0.80 and 0.52, respectively. A value of 1.0 would show the hydrocarbon localized entirely between the methyl group layers; lower values indicate penetration into the surfactant palisade. The numbers 0.94, 0.80 and 0.52 show the hydrocarbon to penetrate more into the space between the surfactant hydrocarbon chains with increased content of SDS. The repulsion between charged headgroups is probably a factor in the penetration of hydrocarbon. The corresponding numbers for the TGDE combination (Table 1) are 0.74, 0.85 and 0.92, and show the opposite trend. Hence, in the combination with TGDE, an increased amount of SDS gave reduced penetration of the hydrocarbon from zone C (Fig. 14) to zone B.

Water penetration was of the opposite trend. The TGDE system (Table 1) gave increased water penetration for enhanced SDS content with hydrocarbon present, while the TEGNPE combination (Table 2) gave not only a reduced penetration, but a negative one.

It is certainly reasonable that penetration by water should prevent penetration by the hydrocarbon and *vice versa*. However, the negative penetration of water in the TEGNPE system (Table 2), may deserve an explanation. A negative penetration means that the interlayer spacing is increased more than what corresponds to the substance added with no penetration. One explanation is that the addition of water causes the expulsion of hydrocarbon from site B to enter site C (Fig. 14) to an extent that the expelled volume exceeds that of the penetrating water. This explanation is supported by the following estimation. The d_0 value is 26.3, independent of the SDS/TEGNPE ratio (Table 2). The volume ratio of the composition SDS/TEGNPE/Isopar M (50:25:25), is equal to 47:23.5:29.5. The penetration fraction α is calculated directly as follows:

$$[(1 - \alpha)29.5]/70.5 = [35.0 - 26.3]/26.3 \text{ and } \alpha = 0.21$$

Hence, $0.21 \times 29.5 = 6.20\%$ is the maximum contribution possible from the hydrocarbon located between the hydrocarbon chains of the surfactant. Maximum water added (Fig. 11) is 33% by volume. The penetration of water is -0.177 , which means that $0.177 \times 33\% = 5.84\%$ of hydrocarbon must leave the penetrated state to enter the space between the methyl group layers. The penetrated hydrocarbon amount is 6.20%, and the water negative penetration of 17.7% is realistic. However, almost all (94%) of the hydrocarbon must be removed from its penetration site between the amphiphilic chains.

PHASE DIAGRAMS OF WATER AND SDS

The enhanced penetration of water with the SDS/non-ionic surfactant ratio for the PGDE, I and TEGNPE systems is an expected feature, because of the repulsion between the ionic surfactants and strong interaction between water molecules and the ionic polar groups.

ACKNOWLEDGMENTS

This research was financially supported by the New York State Commission for Science and Technology through its CAMP program at Clarkson University.

REFERENCES

1. Scamehorn, J.F. (ed.), *Phenomena in Mixed Surfactant Systems*, ACS Symposium Series Vol. 311, American Chemists Society, Washington, D.C., 1986.
2. Rathman, J.F., and J.F. Scamehorn, *J. Phys. Chem.* 88:5807 (1984).
3. Dunn, R.O., J.F. Scamehorn and S.D. Christian, *Sys. Sci. Technol.* 20:257 (1985).
4. Scamehorn, J.F., R.T. Ellington, S.D. Christian, B.W. Penney, R.O. Dunn and S.N. Bhat, *AIChE Symp. Ser.* 250:48 (1986).
5. Hua, S.Y., and M.J. Rosen, *J. Colloid Interface Sci.* 90:2312 (1982).
6. Rosen, M.J., and B.Y. Zhu, *Ibid.* 99:427 (1984).
7. Zhu, B.Y. and M.J. Rosen, *Ibid.* 99:435 (1984).
8. Sagitani, H., and S.E. Friberg, *J. Disp. Sci. Technol.* 1:151 (1980).
9. Sagitani, H., and S.E. Friberg, *Bull. Chem. Soc., Japan* 56:31 (1983).
10. Sjöblom, J., H. Söderlund, S. Lindblad, E.J. Johansen and I.M. Skjarvo, *Colloid P.S.* 268:389 (1990).
11. Sjöblom, J., O. Urdahl, H. Höiland, A.A. Christie and E.J. Johansen, *Progr. Colloid P.S.* 82:131 (1990).
12. Saeten, J.O., J. Sjöblom and B. Gestblom, *J. Phys. Chem.* 95:1449 (1991).
13. Ward, A.J., H. Ku, M.A. Phillippi and C. Marie, *Mol. Cryst. Liq. Cryst.* 154:55 (1988).
14. Ekwall, P., in *Advances in Liquid Crystals* (edited by G.H. Brown) Vol. 1, Academic Press, New York, 1975, p. 1.

[Received November 16, 1990; accepted April 6, 1992]